Available online at www.sciencedirect.com

SCIENCE DIRECT®

Journal of Organometallic Chemistry 672 (2003) 77–85

Journal of Organo metallic Chemistry

www.elsevier.com/locate/jorganchem

Heteronuclear bonding between heavier Group 14 elements and transition-metals: novel halogermylene- and stannylene transition-metal complexes $L^2(X)MM'L'_n$ [L^2 = PhNC(Me)CHC(Me)NPh; X = Cl, I; M = Ge, Sn; $M'L'_n = W(CO)_5$, $Fe(CO)_4$]

Isabelle Saur [a], Ghassoub Rima [a], Karinne Miqueu [b], Heinz Gornitzka [a], Jacques Barrau [a,*]

[a] *Hétérochimie Fondamentale et Appliquée, UMR 5069, Université Paul Sabatier, 118, route de Narbonne, F-31062 Toulouse Cedex 4, France*

[b] *Laboratoire de Physico-Chimie Moléculaire, UMR 5624, Université de Pau et des Pays de l'Adour Av. de l'Université, BP 1155, F-64013 Pau Cedex, France*

Received 20 January 2003; received in revised form 20 January 2003; accepted 26 February 2003

Abstract

Reactions of the stable heteroleptic halodivalent species $L^2(X)M$ [L^2 = PhNC(Me)CHC(Me)NPh; M = Ge, X = Cl (**1**); X = I (**2**); M = Sn, X = Cl (**5**)] with the intermediate metal complexes $W(CO)_5$ THF and $Fe(CO)_4$ have provided the new halogermylene- or stannylenetungsten- and iron-complexes $L^2(X)MM'L'_n$ [$M'L'_n = W(CO)_5$, M = Ge, X = Cl (**3**), X = I (**4**); $M'L'_n = Fe(CO)_4$, X = Cl, M = Ge (**6**), M = Sn (**7**)] respectively; complexes **3**, **4** and **6**, **7** have been characterized via X-ray crystallography and a detailed discussion of their structures is presented. All the MM′ bonds are very short but calculations are consistent with the L^2MX ligands being good σ-donors and very poor π-acceptors in complexes **3**, **4** and **6**, **7**. Selective metathesis reaction between **3** and MeLi resulted in the formation of the stable monomeric complex $L^2(Me)GeW(CO)_5$ (**8**).

Keywords: Transition-metal complexes of M_{14} divalent species; Germanium; Tin; Tungsten; Iron

1. Introduction

The transition-metal complexes, with formal multiple bonding between the metal M′ and the heavier Group 14 element M, have attracted much interest in the past decade because these metallic analogues of carbenic transition-metal complexes are involved as intermediates in the transition metal-catalyzed reactions of formation and/or cleavage of M–C and M–M bonds [1]. Various $R_2MM'L'_n$ structures with three-, four- or five-coordinate M atoms have been isolated to date [2]; but it is noteworthy that the germylenetungsten complex $(\eta^2\text{–}Me_5C_5)(Cl)GeW(CO)_5$ is the unique known example of an heteroleptic halogermylene transition-metal complex [3]. Among the attractive features of such halogen-bound organometallic compounds $L(X)MM'L'_n$ [X = halogen], they appear to be precursors to various alkylated $L(R)GeM'L'_n$ complexes. They thus offer the possibility to modulate the effect that the R moiety has on the nature of the MM′ bond and on the lability of the complexes. These properties can be exploited in catalytic systems. We have previously studied various transition-metal complexes of stable homoleptic Schiff base and phenoxy divalent Group 14 element species, $L_2MM'(CO)_5$, $L_2MM'(CO)_4$ and $(L_2M)_2M'(CO)_4$ [L_2 = 2,2′-*N,N′*-bis(salicylidene)ethylenediamine, (R,R)-(−)-*N,N′*-bis(3,5-di-*tert*-butylsalicylidene)-1,2-cyclohexanediamine, and *N*-methyl-2,2′-iminobis(8-hyhroxyquinoline); M = Ge, Sn, Pb; M′ = Cr, W, Fe. L = 2,4,6-tris[(dimethylamino)methyl]phenyl-; M = Ge, Sn, Pb; M′ = Cr, W, Fe, Pt] [2o,4]. To learn more about the nature of metal–germylene and –stannylene bonding interactions we have used the stable heteroleptic divalent

---

* Corresponding author. Tel.: +33-561-556172; fax: +33-561-558204.

E-mail address: barrau@chimie.ups-tlse.fr (J. Barrau).

0022-328X/03/$ - see front matter © 2003 Elsevier Science B.V. All rights reserved.
doi:10.1016/S0022-328X(03)00144-X

germanium(II) and tin(II) species supported by chelating β-diiminate ligand, $L^2(X)M$ [$L^2 = PhNC(Me)CHC(Me)NPh$, X = Cl, M = Ge (**1**), Sn (**5**); X = I, M = Ge (**2**)], as precursors of the first—except (η^2-Me_5C_5)(Cl)GeW$(CO)_5$—halide complexes $L^2(X)M$-$M'L'_n$ [$M'L'_n = W(CO)_5$; M = Ge; X = Cl (**3**), X = I (**4**). $M'L'_n = Fe(CO)_4$; X = Cl; M = Ge (**6**), Sn (**7**)]. We report here the syntheses, crystal structures and some chemical properties of these new bimetallic compounds. The nature of the M–M′ bonds in these species is discussed in terms of σ-donor and π-acceptor properties of the $L^2(X)M$ ligands toward the M′ atoms. Preliminary results of this work have been communicated earlier [5]. It was reported that $L^2(Cl)M$ three-coordinate divalent species have also been used recently as precursors of the corresponding 'halogermanechalco-genones' $L^2(Cl)GeY$ (Y = S, Se), the first examples of formally multiply-bonded heavier Group 14 elements bearing a halogen [5a,6].

2. Results and discussion

2.1. Complexes $L^2(X)GeW(CO)_5$ (X = Cl (3), I (4))

The reaction of THF solution of the $L^2(X)Ge$ germylenes **1** and **2** [X = Cl (**1**); X = I (**2**)] with the photochemically produced $W(CO)_5 \cdot THF$ intermediate gave the expected dinuclear germylenetungsten complexes $L^2(X)GeW(CO)_5$ [X = Cl (**3**); X = I (**4**)] in high yields (Scheme 1).

Complexes **3** and **4** are yellow solids, soluble in polar or aromatic solvents and insoluble in pentane; they are air- and moisture-sensitive. They were fully characterized by ^1H- and ^{13}C-NMR, IR and mass spectroscopy. These complexes show high thermal stability, as indicated by the high melting point and the presence of the molecular ion peak in the EI 70 eV mass spectrum of **3** (the 100% intensity peak can be attributed to L^2Ge^+). It is noteworthy that the mass spectroscopy analysis of **4**, which bears the weakly coordinating anion I^-, does not show detectable molecular ion peak in this case; the prominent peak being $[L^2Ge]^+$. Mass spectra of both **3** and **4** likewise display the fragmentation patterns of these structures (successive losses of the halides and the carbonyl groups). For **3** and **4** the ^1H- and ^{13}C-NMR spectra show the equivalences of the methyl, and phenyl groups of the ligand as in the cases of the parent germylenes **1** and **2** [5a]. These results are indicative of a mirror symmetry for the ligand in solution. The ^1H and ^{13}C chemical shifts of the methine and methyl groups for **3** appear significantly downfield compared to the corresponding resonances due to the equivalent protons of the divalent species **1** (this feature is less obvious for **4** compared to **2**) (Table 1); similarly the methine ^1H- and ^{13}C-NMR resonances in **4** are strongly shifted downfield in comparison to **3**. This deshielding is consistent with an increased positive charge at the germanium center (or on the L^2Ge ligand) (Table 1). Two ^{13}C-NMR resonances for the CO groups, and three bands in the IR spectra, which can be attributed to the infrared-active carbonyl stretching frequencies ($A_1^{(1)} + A_1^{(2)} + E$), are characteristic of C_{4v} local symmetries around the tungsten in **3** and **4** (Table 1). Since the unique CO_{ax} to the germanium is involved in the $A_1^{(1)}$ mode, the position of this band [1984 (**3**), 1984 (**4**) cm^{-1}] seems indicative of a π-acceptor ability of the $L^2(X)Ge$ groups *trans* to the axial carbonyl [7]. The structures of **3** and **4**

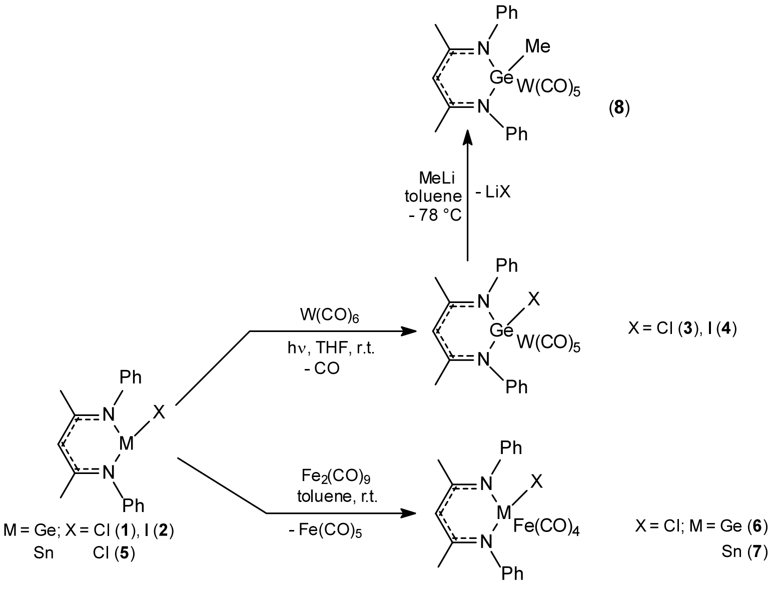

Scheme 1. Synthesis of complexes (**3**–**4**) and (**6**–**7**).

Table 1
^{1}H- and ^{13}C-{^{1}H}-NMR($CDCl_3$) and IR data for compounds **1**, **2**, **3**, **4**

	1 [a]	**2** [a]	**3**	**4**
^{1}H-NMR (δ, ppm)				
CH	5.40	5.64	5.56	5.82
CH_3	1.99	2.05	2.02	2.01
^{13}C-NMR (δ, ppm)				
CH	101.50	103.28	101.58	103.04
CH_3	23.52	23.34	24.60	24.55
CO	–	–	195.88, 199.22	196.58, 199.32
IR	–	–		
ν_{CO} (cm^{-1})	–	–	2072, 1984, 1943	2071, 1984, 1945

[a] Ref. [5].

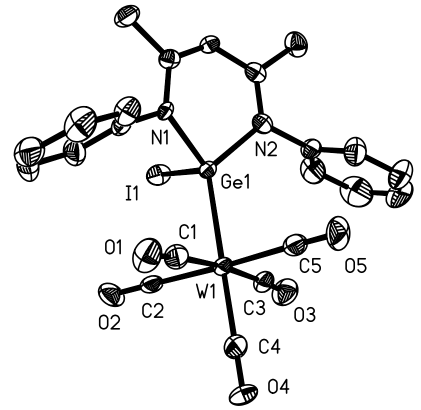

Fig. 2. Crystal structure of **4** (ellipsoids are drawn 50% probability level). Selected bond lengths (Å) and bond angles (°): Ge–I 2.653(1), Ge–N1 1.915(5), Ge–N2 1.916(5), Ge–W 2.571(7), W–C4 1.978(8), W–C1 2.047(8), W–C2 2.027(6), W–C3 2.040(8), W–C5 2.028(7), N1–Ge–N2 93.9(2), N1–Ge–I 97.13(15), N2–Ge–I 95.84(14), N1–Ge–W 125.94(15), N2–Ge–W 125.41(17), I–Ge–W 111.75(2), Ge–W–C4 174.2(3), Ge–W–C1 96.11(19), Ge–W–C2 85.96(17), Ge–W–C3 88.5(2), Ge–W–C5 93.10(18).

were unambiguously established by single-crystal X-ray diffraction. Suitable crystals of **3** and **4** were obtained in chloroform at −78 °C. The molecular structures of **3** and **4** are depicted in Figs. 1 and 2. Crystallographic data are given in Table 2. The molecular structures of **3** and **4** confirm the monomeric nature of these complexes and the four-coordinated environment of the germanium centers; both **3** and **4** have severely distorted tetrahedral geometries around the germanium, with the sums of the angles at the metal center deviating from the sp^{3} tetrahedral value [the sums of the N(1)–Ge–N(2), N(1)–Ge–X, X–Ge–W, N(2)–Ge–W bonds angles are 427.6° (**3**) and 428.2° (**4**)]. The N(1)–Ge–N(2) angles observed in the four-coordinate complexes **3** and **4** [93.9° (**3**), 93.9° (**4**)] are wider than those observed in the three-coordinate germylenes L^{2}(X)Ge [90.3° (**1**), 91.8° (**2**)] [5b], probably due to the change of coordination number of the germanium centers (tricoordinate for **1** and **2** and tetracoordinate for **3** and **4**). The Ge–N and Ge–X bonds in complexes **3** and **4** [Ge–N: 1.929(3), 1.923(3) Å (**3**); 1.916(5), 1.915(5) Å (**4**). Ge–X: 2.258(1) Å (**3**); 2.653(1) Å (**4**)] are slightly shorter than those in divalent species **1** and **2**, respectively [Ge–N: 1.955(2), 1.965(1) Å (**1**); 1.959(4), 1.971(4) Å (**2**). Ge–X: 2.340(6) Å (**1**); 2.778(6) Å (**2**)]. These differences may be ascribable to the diminished electronic densities around the germanium in **3** and **4** compared to **1** and **2**. Moreover, the Ge–X bonds for **3** and **4** are longer by ~0.12 Å than those for more basic corresponding halogenated germanium(IV) compounds [8]. All these data are consistent with geometries around the germanium centers in **3** and **4** that are in fact between distorted trigonal pyramids and tetrahedrons (see side views, Fig. 3).

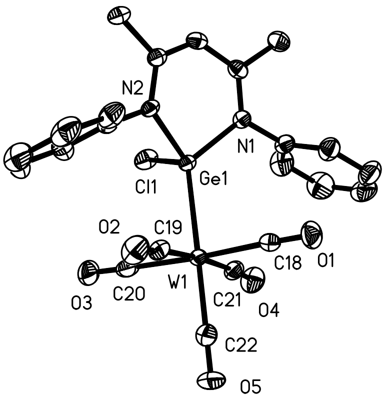

Fig. 1. Crystal structure of **3** (ellipsoids are drawn 50% probability level). Selected bond lengths (Å) and bond angles (°): Ge–Cl 2.258(1), Ge–N1 1.929(3), Ge–N2 1.923(3), Ge–W 2.567(5), W–C22 1.995(5), W–C18 2.033(4), W–C21 2.035(5), W–C19 2.040(5), W–C20 2.043(4), N1–Ge–N2 93.90(13), N1–Ge–Cl 96.64(9), N2–Ge–Cl 98.08(10), N1–Ge–W 124.97(9), N2–Ge–W 124.73(10), Cl–Ge–W 112.34(3), Ge–W–C22 174.83(14), Ge–W–C18 92.11(11), Ge–W–C21 89.50(12), Ge–W–C19 95.49(12), Ge–W–C20 85.79(11).

In both complexes **3** and **4**, the geometry around the tungsten is nearly octahedral (Figs. 1 and 2). The Ge–W bond lengths [2.567(5) Å (**3**), 2.571(7) Å (**4**)] are nearly identical to those observed for (η^{2}-Me_5C_5)(Cl)-$GeW(CO)_5$ [2.571(1) Å] [3] and for various halogermanium(IV) complexes (η^{5}-C_5R_5)$M(CO)_3GeCl_3$ (R = H, Me; M = Mo, W) [8c,8d,8e]. They are among the shortest reported for compounds of $R_2GeW(CO)_5$ type [2i,2m,2q,2r,9]; and even shorter than the Ge=W bond length of 2.593(1) Å determined for Ar^{1}Ar^{2}Ge=W(CO)$_5$ [Ar^{1} = 2,4,6-tris[bis(trimethylsilyl)methyl]phenyl, Ar^{2} = 2,4,6-triisopropylphenyl] in which the germanium atom is three-coordinated [2i]. The range for an interatomic Ge–W single bond is 2.59–2.67 Å [2m,2q,10]. It is noteworthy that in the two complexes the W–C$_{ax}$ bonds [1.995(5) Å (**3**); 1.978(8) Å (**4**)] are slightly shorter than the W–C$_{eq}$ bonds [~2.038 Å (**3**); ~2.035 Å (**4**)] and are the largest among the W–C$_{ax}$

Table 2
Crystallographic Data for **3**, **4**, **6**, **7**

Compounds	**3**	**4**	**6**	**7**
Empirical formula	$C_{22}H_{17}ClGeN_2O_5W$	$C_{22}H_{17}IGeN_2O_5W$	$C_{21}H_{17}ClFeGeN_2O_4$	$C_{21}H_{17}ClFeN_2O_4Sn$
Formula weight	681.27	772.72	525.26	571.36
Crystal system	orthorhombic	orthorhombic	orthorhombic	orthorhombic
Space group	$P2_12_12_1$	$P2_12_12_1$	$P2_12_12_1$	*Pnma*
Unit cell dimensions				
a, (Å)	6.684(1)	6.860(1)	12.232(10)	13.420(7)
b, (Å)	17.959(2)	18.405(2)	13.230(6)	14.170(9)
c, (Å)	19.508(2)	19.620(2)	13.714(7)	12.001(7)
V, (Å^3)	2341.6(4)	2477.1(5)	2219(2)	2282(2)
Z	4	4	4	4
D_{calc}, (Mg m^{-3})	1.932	2.072	1.572	1.663
Reflections collected	19708	20974	12888	12710
Independent reflections	5796	6402	4474	2458
Parameters	291	291	273	234
R_1 [$I > 2\sigma(I)$]	0.0236	0.0370	0.0216	0.0239
wR_2 (all data)	0.0502	0.0835	0.0466	0.0560
Largest difference peak and hole (e. Å^{-3})	1.330 and −0.968	2.071 and −1.859	0.390 and −0.275	0.420 and −0.350

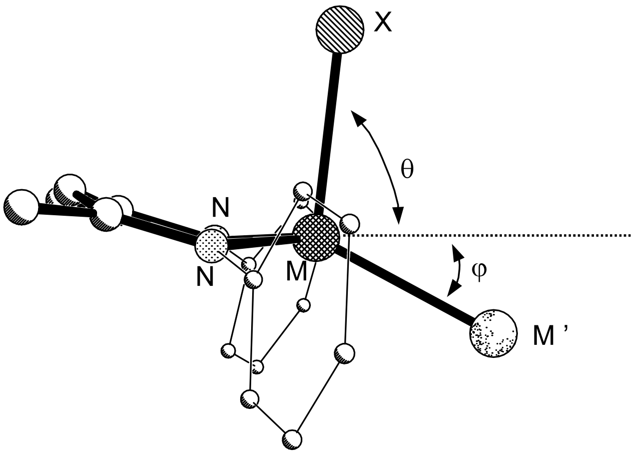

Compounds	$L^2(Cl)GeW(CO)_5$ (**3**)	$L^2(I)GeW(CO)_5$ (**4**)	$L^2(Cl)GeFe(CO)_4$ (**6**)	$L^2(Cl)SnFe(CO)_4$ (**7**)
80.5	79		77.5	80
φ (°)	33	31	42	42

Fig. 3. Side view of **3**, **4**, and **6**, **7**. CO groups are omitted for clarity.

bonds yet observed in germylenetungsten complexes [2i,2m,2q,2r,9]. All these data seem indicative of Ge–W bonds with unsaturated character (hyperconjugation [8c,8d,8e]). Accordingly the $L^2(X)Ge$ moiety could be seen, toward the $W(CO)_5$ moiety, as strong σ-donors with weak π-acceptor capacities; nevertheless the π contributions in these germanium–tungsten compounds seem less lower than those in the few known base-stabilized germylene–pentacarbonyltungsten complexes [2m,2q,2r,9].

Table 3
Geometrical parameters (bond lengths in angstroms and bond angles in degrees) and Wiberg Bond Indices in parenthesis

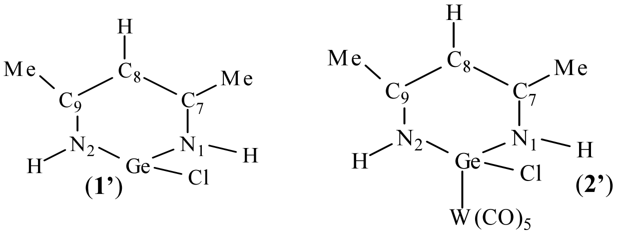

	1′	**2′**
GeCl	2.343 (0.640)	2.267 (0.688)
GeN_1	1.994 (0.474)	1.931 (0.481)
GeN_2	1.994 (0.474)	1.933 (0.480)
N_1C_7	1.344 (1.404)	1.347 (1.379)
C_7C_8	1.422 (1.364)	1.420 (1.371)
C_9C_8	1.422 (1.364)	1.421 (1.370)
N_2C_9	1.344 (1.405)	1.347 (1.380)
GeW	–	2.607 (0.455)
N_1GeN_2	86.84	90.39
N_1GeCl	95.90	98.38
N_2GeCl	95.84	98.30
WGeCl	–	122.24

In order to estimate the overall bonding situation of the L_2GeX ligand in these germanium(II)–tungsten complexes a DFT(B3LYP) theoretical study was carried out for the model (without phenyl substituents) molecules **1′** and **2′**. The calculated geometrical parameters of **1′** and **2′** (Table 3) are in good qualitative agreement with the experimental results. For **1′**, the calculated hybrid orbitals (NBO calculation) of the Ge atom for the Ge–N and Ge–Cl bonds are p in character (92.86 and 93.48%, respectively); the lone pair presents a strong s character (83.16%). On the contrary, for **2′** the Ge–N and Ge–Cl bonds correspond to a $sp^{2.6}$ hybridized germanium atom. Consequently, a shortening of the Ge–Cl and Ge–N bonds as well as an increase of the N(1)GeN(2) and N(1,2)GeCl bond angles are predicted going from the free ligand L_2Ge **1′** to the L_2Ge fragment

Table 4
Total natural charge (NBO calculation)

	1′	**2′**
Ge	1.045	1.392
N_1	−0.940	−0.947
N_2	−0.939	−0.946
Cl	−0.592	−0.498
C_7	0.387	0.396
C_8	−0.402	−0.393
C_9	0.387	0.396
W	/	−1.228

in **2′**. The germanium pair of the Ge–W bond presents a strong p character (82.66%). This observation could explain the short Ge–W bond in **2′**. Moreover, taking into account the energetic positions of the π^*_{CN} (−1.46 eV), σ^*_{GeN} (0.13 eV) and σ^*_{GeCl} (0.27 eV) orbitals of the L_2GeCl fragment and of the d orbital (π symmetry) in $W(CO)_5$ (−6.82 eV), it appears that only a very weak back-donation $d_M \rightarrow$ligand could occur. This bonding situation is witnessed in the Wiberg bond indices (Table 3). Considering the total atomic natural charges (Table 4) for **1′** and **2′**, it appears that (i) the C_8 atom is less negative in **2′** than in **1′**, which is in agreement with the deshielding observed in ^{13}C- and ^{1}H-NMR, (ii) the chlorine atom is slightly less negative in the complex **2′** than in the free ligand **1′**, (iii) the germanium atom is strongly positive in **2′** versus in **1′**, and (iv) the tungsten presents a more important charge in **2′** (−1.228) than in the free fragment $W(CO)_5$ (−0.690). These charges are coherent with a weak back-donation $d_M \rightarrow$ligand.

In conclusion, these trends can be rationalized assuming a rehybridization of the germanium atom going from the free ligand L^2GeCl (**1′**) to the complex **2′**, the Ge–W bonding being achieved essentially by a strong σ donor–acceptor interaction. A tungsten to germanium π back-donation ($d_M \rightarrow \sigma^*_{GeCl}$, $d_M \rightarrow \sigma^*_{GeN}$) is possible but seems weak.

2.2. *Complexes $L^2(Cl)MFe(CO)_4$ (M = Ge (6), Sn (7))*

The germylene- and stannylene- iron complexes $L^2(Cl)MFe(CO)_4$ [M = Ge (**6**), Sn (**7**)] were synthesized by reaction of diiron nonacarbonyl with the corresponding divalent species $L^2(Cl)M$ [M = Ge (**1**), Sn (**5**)] in toluene at room temperature (Scheme 1). Complexes **6** and **7** were obtained as yellow solids, in high yields, after precipitation in pentane. As for **3** and **4**, these air- and moisture-sensitive complexes are soluble in aromatic and polar solvents. Their ^{1}H, ^{13}C-NMR, IR and mass spectra are consistent with their formula (Table 5).

Table 5
^{1}H- and ^{13}C-{^{1}H}-NMR($CDCl_3$) and IR data for compounds **5**, **6**, **7**

	5 [a]	**6**	**7**
^{1}H-NMR (δ, ppm)			
CH	5.15	5.50	5.31
CH_3	1.96	1.97	2.03
^{13}C-NMR (δ, ppm)			
CH	100.74	101.18	100.38
CH_3	23.96	24.66	24.56
CO	–	213.14	212.40
IR			
ν_{CO} (cm^{-1})	–	2043, 1969,	2044, 1969,
	–	1947, 1923	1950, 1928

[a] Ref. [5].

The ^{119}Sn NMR signal of **7** at δ = 80.1 ppm, is shifted to low field in comparison to the signal of the parent stannylene **5** [5a] [δ = −280 ppm], indicating that the tin atom in **7** is basically four-coordinate in solution. The deshielding also affects the ^{1}H- and ^{13}C-NMR chemical shifts of the signals of complex **7**, compared to those of the free divalent species **5** (Table 5). Though this is the expected result for the higher coordination number of Sn in **7**, this feature is less obvious for **6**. The ^{1}H and ^{13}C chemical shifts of **6** are in the range of those of **3**, but are slightly shifted to high field indicating a smaller electron-withdrawing ability for $Fe(CO)_4$ than for $W(CO)_5$ (Tables 1 and 5). The IR spectra of both complexes **6** and **7** exhibit four carbonyl bands indicative of a C_{3v} local symmetry at the iron with the ligand $L^2(Cl)M$ in the axial site (Table 5). The structures of **6** and **7** were unambiguously established by single-crystal X-ray analyses and are shown in Figs. 4 and 5, respectively. Crystallographic data and processing parameters are given in Table 2.

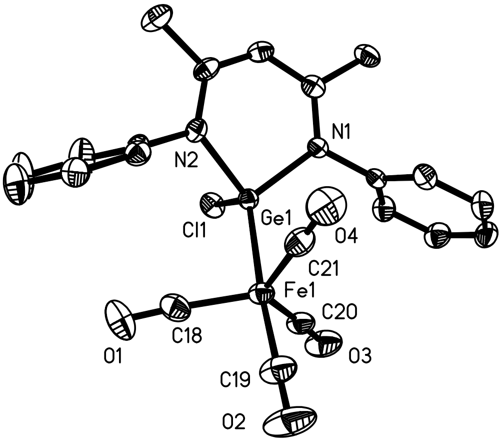

Fig. 4. Crystal structure of **6** (ellipsoids are drawn 50% probability level). Selected bond lengths (Å) and bond angles (°): Ge–Cl 2.245(13), Ge–N1 1.911(2), Ge–N2 1.912(2), Ge–Fe 2.298(2), Fe–C19 1.790(3), Fe–C18 1.790(3), Fe–C20 1.795(3), Fe–C21 1.785(3), N1–Ge–N2 94.59(8), N1–Ge–Cl 98.31(7), N2–Ge–Cl 98.54(6), N1–Ge–Fe 119.95(6), N2–Ge–Fe 120.94(6), Cl–Ge–Fe 119.17(5), Ge–Fe–C19 175.40(10), Ge–Fe–C18 91.50(8), Ge–Fe–C20 88.86(8), Ge–Fe–C21 84.28(8).

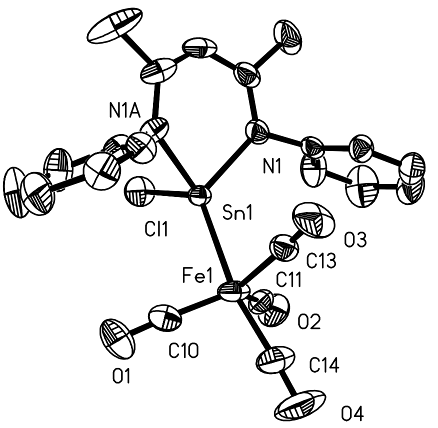

Fig. 5. Crystal structure of **7** (ellipsoids are drawn 50% probability level). Selected bond lengths (Å) and bond angles (°): Sn–Cl 2.394(1), Sn–N1 2.091(2), Sn–N1A 2.091(2), Sn–Fe 2.440(1), Fe–C14 1.801(5), Fe–C10 1.649(14), Fe–C11 1.926(13), Fe–C13 1.800(5), N1–Sn–N1A 89.35(13), N1–Sn–Cl 97.02(6), N1A–Sn–Cl 97.02(6), N1–Sn–Fe 121.90(6), N1A–Sn–Fe 121.90(6), Cl–Sn–Fe 122.10(4), Sn–Fe–C14 167.7(2), Sn–Fe–C10 94.9(5), Sn–Fe–C11 85.3(5), Sn–Fe–C13 85.94(14).

These two complexes have similar structural features. The backbone of the L^2 ligand is essentially planar; as for **3** and **4**, the metal 14 atom center adopts a four-coordinated geometry and resides in an environment intermediate between a distorted tetrahedron and a trigonal pyramid (see side view, Fig. 3), while the local geometry around the iron center is slightly distorted trigonal bipyramidal. In the two complexes the L^2(X)M moiety occupies an axial position in the trigonal bipyramid. This indicates that the divalent species L^2(Cl)M are better σ-donors than π-acceptors toward iron in accord with theoretical studies showing that the axial or equatorial sites preference of a neutral ligand in trigonal bipyramidal d^8 metal(0) carbonyl complexes can depend on the σ-donor and π-acceptor characters of this ligand, the *eq*-preference being attributed to ligands having good π-acceptor character [11,12b]. As expected due to the difference of the atomic radii of Ge and Sn, the bond angle N(1)–Ge–N(2) [94.6°] in **6** is larger than the corresponding angle N(1)–Sn–N(2) [89.4°] in **7**, and the bond lengths N–Ge [1.911(2), 1.912(2) Å] and Ge–Cl [2.245(1) Å] in **6** are slightly shorter than the corresponding N–Sn [2.091(2), 2.091(2) Å] and Sn–Cl [2.394(1) Å] bond distances in **7**. Further, due to the change of the metal 14 atom environments (tetracoordinate in **6**, **7** and tricoordinate in **1**, **5**), these M–N and M–Cl bond distances are shorter in **6**, **7** (Figs. 4 and 5) than the corresponding bond lengths in **1** and **5** [Ge–N: 1.955(2), 1.965(1) Å; Ge–Cl: 2.340(6) Å (**1**). Sn–N: 2.170(9), 2.174(9) Å; Sn–Cl: 2.500(3) Å (**5**)] [5a]. The M–Fe bond distances [Ge–Fe: 2.298(2) Å (**6**); Sn–Fe: 2.440(1) Å (**7**)] are, among the shortest known for any germylene- [2p,12] and stannylene- [2k,4a,12b,13] iron complexes respectively. Additionally the Fe–C_{ax} to the metal [1.790(3) Å (**6**), 1.801(5) Å (**7**)] and the Fe–C_{eq} [~1.790 Å (**6**), ~1.792 Å (**7**)] bonds are almost identical. The only M–Fe distances shorter than those observed in **6** and **7** were determined in the iron complexes of the bis(aryloxy)Group14 metal(II) species $(ArO)_2MFe(CO)_4$ [ArO = 2,6-tBu$_2$-4-Me-C$_6$H$_2$–O; M = Ge (2.240(2) Å), Sn (2.408(1) Å)] in which the $(ArO)_2M$ ligands are in equatorial positions due to the good π-acceptor character of these $(ArO)_2M$ ligands [12b]. Three arguments support the view that the L^2(Cl)M ligands are strong σ-donors probably in weak hyperconjugation with the carbonyl iron fragment: (i) the M–Fe bonds in **6** and **7** are shorter than those found in most complexes containing a tetracoordinated metal 14 atom [2k,2p,4a,12a,12c,12d,13a,13b,13c], (ii) the M′–C distances are very similar, (iii) the $L^2(Cl)MFe(CO)_4$ complexes have trigonal bipyramidal *trans* configurations at the iron. It is noteworthy that **6** and **7** are the first group 8 transition-metal complexes of heavier Group 14 element divalent species bearing a halogen.

2.3. Chemical reactivity

These heteroleptic divalent transition-metal complexes $L^2(X)MM'L'_n$ present a large potential for organometallic syntheses since six different reaction centers can be distinguished. But the widespread interest in the chemistry of these compounds is essentially due to the presence of a halogen on the M atom offering suitable approaches to numerous unusual new complexes. The reactivity of **3** was preliminary studied with MeLi. The reaction of **3** with MeLi in toluene at −78 °C is selective and almost quantitative, leading to the complex $L^2(Me)GeW(CO)_5$ **8** that has been characterized by ^{1}H- and ^{13}C-NMR, IR and mass spectrum. The thermal stability of this complex is revealed by the presence of a prominent peak corresponding to the molecular ion in the EI mass spectrum. In the IR spectra, the absorption bonds attributed to the carbonyl frequencies are at lower wavenumbers for complex **8** [**8**: 2060, 1934, 1920 cm^{-1}] than for complex **3** [**3**: 2072, 1984, 1943 cm^{-1}], probably due to the difference of the electronic effects of the chlorine and methyl substituents.

3. Conclusion

Four members of a new class of complexes, the halogermylene- and stannylene- transition-metal complexes $L^2(X)MM'L'_n$, have been described. The MM′ bond distances in these complexes are among the shortest ever observed. Calculations indicate that the L^2(X)M ligands are strong σ-donors that possess low π-acceptor properties (hyperconjugation) toward the $M'L_n$ fragment. Thus if these compounds are described

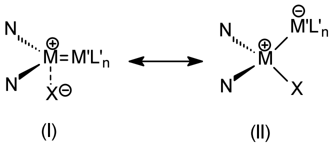

Scheme 2. Resonance structures of complexes (**3**–**4**) and (**6**–**7**).

in terms of resonance structures between forms containing Group 14 element-transition metal double bonds and ylid forms, (as shown in Scheme 2, considering that the parent compounds **1**, **2**, and **5** are well described as $L^2M^+\ldots X^-$ species [5b]), the ylid forms(II) are by far the major resonance contributors to the actual structures of the M_{14}–M′ bonds.

These complexes, by virtue of their polar metal 14-transition metal and their metal 14-halogen bonds, appear as useful precursors with high potential in organometallic chemistry. They offer diverse uses to develop, via replacement of the chlorine by a more labile ligand, abstraction of the halogen to afford cationic metal(II) complexes, and selective substitution of the halogen for preparation of complexes containing alkyl groups.

4. Experimental

4.1. General procedures and materials

All manipulations were carried out under an argon atmosphere with the use of standard Schlenk and high vacuum line techniques. Solvents were distilled from conventional drying agents and degassed twice prior to use [14]. $L^2(X)M$ [M = Ge, X = Cl (**1**), I (**2**); M = Sn, X = Cl (**5**)] were prepared according to the previously reported method [5a]. ^{1}H-NMR spectra were recorded on a Bruker AC 80 spectrometer operating at 80 MHz (chemical shifts are given in ppm (δ) relative to Me_4Si), ^{13}C spectra on a AC-200 MHz spectrometer operating at 62.9 MHz; the multiplicity of the ^{13}C-NMR signals was determined by the APT technique. ^{119}Sn{^{1}H} NMR spectra were recorded on a Bruker AC-200 or 400 MHz (spectrometer frequency 74.63 or 149.21 MHz, chemical shifts are reported in ppm (δ) relative to external Me_4Sn). Mass spectra were recorded on a Nermag R10-10H or a Hewlett Packard 5989 instrument operating, in the electron impact mode at 70 eV and samples were contained in glass capillaries under argon. IR spectra were obtained on a Perkin–Elmer 1600 FT-IR. Irradiations were carried out at 25 °C by using a low-pressure mercury immersion lamp in a quartz tube. Melting points were taken on a hot-plate microscope apparatus Leitz Biomed. Elemental analyses (C, H, N) were performed at the ‘Microanalysis Laboratory of the Ecole Nationale Supérieure de Chimie de Toulouse’.

4.2. $L^2(Cl)GeW(CO)_5$ (3)

A tetrahydrofuran solution (60 ml) of $W(CO)_6$ (440 mg, 1.25 mmol) was irradiated for 2 h. CO was eliminated by bubbling of argon in the reaction mixture for 15 min, then L^2GeCl (450 mg, 1.25 mmol) in tetrahydrofuran (30 ml) was slowly added at room temperature. The mixture was stirred for 2 h. The volatile materials were removed under reduced pressure to obtain **3** as a yellow solid (83% yield, 710 mg). Recrystallization from chloroform at −30 °C gave yellow crystals of **3**: mp 190–205 °C (dec.). IR ($CHCl_3$) $\nu = 2072$, 1984, 1943 cm^{-1} (CO). ^{1}H-NMR (80 MHz, $CDCl_3$): $\delta = 2.02$ (s, 6H, CH_3), 5.56 (s, 1H, CH), 7.15–7.56 (m, 10H, C_6H_5). ^{13}C-NMR (62.90 MHz, $CDCl_3$): $\delta = 24.60$ (s, CH_3), 101.58 (s, CH), 128.04 (s, *m*-aryl-C), 128.47 (s, *p*-aryl-C), 130.04 (s, *o*-aryl-C), 142.43 (s, C–N), 167.38 (s, C_{ipso}), 195.88 (s, CO), 199.22 (s, CO). MS: (EI) $m/z = 682$ $[M]^+$, 654 $[M-CO]^+$. [D1]Anal. Calc. for $C_{22}H_{17}N_2O_5ClGeW$, (681.27): C, 38.70; H, 2.49; N, 4.10. Found: C, 38.75; H, 2.17; N, 4.25%.

4.3. $L^2(I)GeW(CO)_5$ (4)

Using the same operating conditions as in the preceding preparation, **4** was obtained from L^2GeI (370 mg, 0.85 mmol) and $W(CO)_5$ THF (360 mg, 0.85 mmol). Yield: 86%, 550 mg. **4**: mp 178–180 °C. IR (THF) $\nu = 2071$, 1984, 1945 cm^{-1}(CO). ^{1}H-NMR (80 MHz, $CDCl_3$): $\delta = 2.01$ (s, 6H, CH_3), 5.82 (s, 1H, CH), 7.18–7.25 (m, 10H, C_6H_5). ^{13}C-NMR (62.90 MHz, $CDCl_3$): $\delta = 24.55$ (s, CH_3), 103.04 (s, CH), 126.42 (s, *m*-aryl-C), 129.67 (s, *p*-aryl-C), 130.02 (s, *o*-aryl-C), 142.40 (s, C–N), 168.76 (s, C_{ipso}), 196.58 (s, CO), 199.32 (s, CO). MS: (EI) $m/z = 645$ $[M-I]^+$, 617 $[M-I-CO]^+$. Anal. Calc. for $C_{22}H_{17}N_2O_5IgeW$, (772.72): C, 34.19; H, 2.22; N, 3.63. Found: C, 34.03; H, 2.27; N, 3.66%.

4.4. $L^2(Cl)GeFe(CO)_4$ (6)

A toluene solution (10 ml) of L^2GeCl (290 mg, 0.81 mmol) was slowly added to a suspension of $Fe_2(CO)_9$ (300 mg, 0.81 mmol) in toluene (20 ml). The reaction mixture was then stirred at room temperature for 24 h. The volatile materials were removed in vacuo, the residue was dissolved in chloroform (5 ml) and the solution was cooled at −30 °C to give **6** (91%, 390 mg) as yellow crystals. **6**: mp 200–202 °C (dec.). IR ($CHCl_3$) $\nu = 2043$, 1969, 1947, 1923 cm^{-1}(CO). ^{1}H-NMR (80 MHz, $CDCl_3$): $\delta = 1.97$ (s, 6H, CH_3), 5.50 (s, 1H, CH), 7.15–7.42 (m, 10H, C_6H_5). ^{13}C-NMR (62.90 MHz, $CDCl_3$): $\delta = 24.66$ (s, CH_3), 101.18 (s, CH), 127.65 (s, *m*-aryl-C), 129.34 (s, *p*-aryl-C), 130.76 (s, *o*-aryl-C), 141.62 (s, C–N), 168.81 (s, C_{ipso}), 213.14 (s, CO). MS: (EI) $m/z = 526$ $[M]^+$, 498 $[M-CO]^+$. Anal. Calc. for

$C_{21}H_{17}N_2O_4ClFeGe$, (525.26): C, 48.02; H, 3.26; N, 5.33. Found: C, 47.85; H, 3.12; N, 5.41%.

4.5. $L^2(Cl)SnFe(CO)_4$ (7)

Following the same experimental procedure as for the synthesis of **6**, the reaction of L^2SnCl (470 mg, 1.17 mmol) with $Fe_2(CO)_9$ (430 mg, 1.17 mmol) in 40 ml of toluene afforded **7** (91%, 610 mg). **7**: mp 132–134 °C (dec.). IR ($CHCl_3$) $v = 2044$, 1969, 1950, 1928 cm^{-1}(CO). ^{119}Sn (149.2 MHz, $CDCl_3$): $\delta = 80$. ^1H-NMR (80 MHz, $CDCl_3$): $\delta = 2.03$ (s, 6H, CH_3), 5.31 (s, 1H, CH), 7.24–7.35 (m, 10H, C_6H_5). ^{13}C-NMR (62.90 MHz, $CDCl_3$): $\delta = 24.56$ (s, CH_3), 100.38 (s, CH), 126.22 (s, *m*-aryl-C), 130.12 (s, *p*-aryl-C), 130.02 (s, *o*-aryl-C), 143.13 (s, C–N), 169.34 (s, C_{ipso}), 212.40 (s, CO). MS (EI) $m/z = 516$ $[M-2CO]^+$. Anal. Calc. for $C_{21}H_{17}N_2O_4ClFeSn$, (571.40): C, 44.47; H, 2.99; N, 4.90. Found: C, 43.90; H, 2.82; N, 4.78%.

4.6. $L^2(Me)GeW(CO)_5$ (**8**)

A toluene solution (10 ml) of $L^2(Cl)Ge = W(CO)_5$ (52 mg, 0.076 mmol) was treated with MeLi (48 µl, 1.6 M ether solution) at −78 °C. After the mixture was warmed to room temperature over 3 h to give a red solution, the solvent was removed under reduced pressure to afford **8** as red solid (80%, 40 mg). This solid was recrystallized from toluene at −30 °C to obtain red crystals of **8**. **8**: mp 170–172 °C. IR ($CHCl_3$) $v = 2060$, 1934, 1920 cm^{-1}(CO). ^1H-NMR (80 MHz, C_6D_6): $\delta = 0.48$ (s, 3H, CH_3), 1.52 (s, 6H, CH_3), 4.84 (s, 1H, CH), 7.02–7.36 (m, 10H, C_6H_5). ^{13}C-NMR (62.90 MHz, C_6D_6): $\delta = 11.23$ (s, CH_3), 22.35 (s, CH_3), 100.97 (s, CH), 126.44 (s, *m*-aryl-C), 127.63 (s, *p*-aryl-C), 128.56 (s, *o*-aryl-C), 143.99 (s, C–N), 166.95 (s, C_{ipso}), 198.03 (s, CO), 200.90 (s, CO). MS (EI) $m/z =$ 660 $[M]^+$, 645 $[M-CH_3]^+$. Anal. Calc. for $C_{23}H_{20}N_2O_5GeW$, (660.85): C, 41.80; H, 3.05; N, 4.24. Found: C, 41.76; H, 2.80; N, 4.18%.

4.7. X-ray measurements

Crystal data for **3**, **4**, **6** and **7** are presented in Table 2. All data were collected at low temperatures (− 80 °C) on a Bruker-AXS CCD 1000 diffractometer with Mo–Kα ($\lambda = 0.71073$ Å). The structures were solved by direct methods by means of SHELXS-97 [15] and refined with all data on F^2 by means of SHELXL-97 [16]. All non-hydrogen atoms were refined anisotropically. The hydrogen atoms of the molecules were geometrically idealized and refined using a riding model. A disorder of the phenyl group in **7** was refined anisotropically on two positions (54/46) with the help of ADP and distances restraints.

4.8. Computational details

Calculations were performed with the GAUSSIAN-98 program [17,18]. The density functional method [19] used was the hybrid exchange functional B3LYP [20]. This functional includes a linear combination of a small amount (20%) of exact exchange with the Becke 88 gradient-corrected exchange [20a] and with the correlation energy functional LYP [20c]

$$E_{xc} = aE_x^{HF} + bE_x^{LDA} + cE_x^{GGA} + dE_c^{LDA} + eE_c^{GGA}$$

Standard parameterization has been retained ($a = 0.20$, $b = 1 - a$, $c = 0.72$ for Becke exchange, $e = 0.81$ for the gradient-corrected part of the correlation energy functional, and $d = 1 - e$).

The basis set retained for all calculations is the relativistically corrected effective core potential of Stevens et al. [21] with a double ζ basis expansion for the valence space [CEP-31G(d)]. All heavy main group atoms were augmented with a single set of polarisation functions. For the germanium, the coefficient used is $\alpha_d^{Ge} = 0.202$ [22]. The optimized structures were confirmed as minima on the potential energy surface by second-derivative calculations. The population analyses at the given optimized geometries (Wiberg bond indices) were carried out according to the Wenhold–Redd partitioning Scheme [23].

5. Supplementary material

Crystallographic data (excluding structure factors) have been deposited with the Cambridge Crystallographic Data Center, CCDC 201526-201529 for **3**, **4**, **6** and **7**. Copies of the data can be obtained free of charge on application to CCDC, 12 Union Road, Cambridge CB2 1EZ, UK (fax: +44-1223-336033; e-mail deposit@ccdc.cam.ac.uk or www: http://www.ccdc.cam.ac.uk).

Acknowledgements

We wish to thank Mrs G. Pfister-Guillouzo for helpful discussions on the analysis of calculations data. We thank the Institut du Developpement de Ressources en Informatique Scientifique (IDRIS, Orsay, France), administered by the CNRS, for the calculation facilities.

References

[1] (a) T. Hayashi, H. Yamashita, M. Tanaka, M. Goto, Organometallics 11 (1992) 3227;
(b) K.H. Pannell, M.C. Brun, H. Sharma, K. Jones, S. Sharma, Organometallics 13 (1994) 1075;
(c) R.H. Heyn, T.D. Tilley, J. Am. Chem. Soc. 114 (1992) 1917;
(d) E.W. Finckh, B.Z. Tang, A. Lough, I. Manners, Organome-

tallics 11 (1988) 2904;

(e) M. Ishikawa, A Naka, S. Okazaki, H. Sakamoto, Organometallics 12 (1993) 87;

(f) J. Lee, C. Lee, S.S. Lee, S.O. Kang, J. Ko, Chem. Commun. (2001) 1730;

(g) Y. Kang, J. Lee, Y.K. Kong, S.O. Kang, J. Ko, Organometallics 19 (2000) 1722 (and references herein).

[2] (a) E. Brooks, H.R. Cros, J. Organomet. Chem. Rev. A 6 (1970) 227;

(b) M. Veith, O. Recktenwald, Top. Curr. Chem. 104 (1982) 1;

(c) W. Petz, Chem. Rev. 86 (1986) 1019;

(d) M.F. Lappert, R.S. Rowe, Coord. Chem. Rev. 100 (1990) 267;

(e) J.T.B. Jastrzebski, G. van Koten, Adv. Organomet. Chem. 35 (1993) 241 (For recent investigation see);

(f) H. Handwerker, C. Leis, R. Probst, P. Bissinger, A. Grohmann, P. Kiprof, E. Herdtweck, J. Blümel, N. Auner, C. Zybill, Organometallics 12 (1993) 2162;

(g) S.L. Ellis, P.B. Hitchcock, S.A. Holmes, M.F. Lappert, J. Slade, J. Organomet. Chem. 444 (1993) 95;

(h) D.A. Atwood, V.O. Atwood, A.H. Cowley, H.R. Gobran, Inorg. Chem. 32 (1993) 4671;

(i) N. Tokitoh, K. Manmaru, R. Okazaki, Organometallics 13 (1994) 167;

(j) M. Weidenbruch, A. Stilter, J. Schlaefke, K. Peters, H.G. von Schnering, J. Organomet. Chem. 501 (1995) 67;

(k) M. Weidenbruch, A. Stilter, K. Peters, H.G. von Schnering, Z. Anorg. Allg. Chem. 622 (1996) 534;

(l) M Weidenbruch, A. Silter, K. Peters, H.G. von Schnering, Chem. Ber. 129 (1996) 1565;

(m) H. Lang, M. Wienmann, W. Fresch, M. Büchner, B. Schiemenz, Chem. Commun. (1996) 1299;

(n) L.K. Figge, P.J. Caroll, D.H. Berry, Angew. Chem. Int. Ed. Engl. 35 (1996) 435;

(o) M. Weidenbruch, A. Stilter, W. Saak, K. Peters, H.G. von Schnering, J. Organomet. Chem. 560 (1998) 125;

(p) J. Barrau, G. Rima, T. El Amraoui, J. Organomet. Chem. 570 (1998) 163;

(q) H. Tobita, K. Ishiyama, Y. Kawano, S. Inomata, H. Ogino, Organometallics 17 (1998) 789;

(r) K. Ueno, K. Yamaguchi, H. Ogino, Organometallics 18 (1999) 4468;

(s) C. Bibal, S. Mazière, H. Gornitzka, C. Couret, Organometallics 21 (2002) 2940.

[3] P. Jutzi, B. Hampel, K. Stroppel, C. Krüger, K. Angermund, P. Hofman, Chem. Ber. 118 (1985) 2789.

[4] (a) D. Agustin, G. Rima, H. Gornitzka, J. Barrau, Inorg. Chem. 39 (2000) 5492;

(b) D. Agustin, G. Rima, H. Gornitzka, J. Barrau, Eur. J. Inorg. Chem. (2000) 693.

[5] (a) A. Akkari, J.J. Byrne, I. Saur, G. Rima, H. Gornitzka, J. Barrau, J. Organomet. Chem. 622 (2001) 190;

(b) I. Saur, K. Miqueu, G. Rima, J. Barrau, A. Chrostowska, V. Lemierre, G. Pfister-Guillouzo, organometallics submitted for publication.

[6] I. Saur, G. Rima, H. Gornitzka, J. Barrau, Organometallics 22 (2003) 1106.

[7] T.J. Marks, J. Am. Chem. Soc. 93 (1971) 7090.

[8] (a) A. Sekigushi, Y. Ishida, N. Fukaya, I. Masaaki, J. Am. Chem. Soc. 124 (2002) 1158;

(b) A.C. Filippou, P. Portius, A.I. Philippopoulos, Organometallics 21 (2002) 653;

(c) A.C. Filippou, P. Portius, G. Winter, G. Kociok-Köhn, J. Organomet. Chem. 628 (2001) 11;

(d) A.C. Filippou, G. Winter, M. Feist, G. Kociok-Köhn, I. Hinz, Polyhedron 17 (1998) 1103;

(e) A.C. Filippou, G. Winter, G. Kociok-Köhn, C. Troll, I. Hinz, Organometallics 18 (1999) 2649.

[9] (a) P. Jutzi, B. Hampel, B.M. Hursthouse, A.J. Howes, J. Organomet. Chem. 19 (1986) 289;

(b) W.W. Du Mont, L. Lange, S. Pohl, W. Saak, Organometallics 9 (1990) 1395;

(c) G. Huttner, U. Weber, B. Sigwarth, O. Scheidstger, H. Lang, L. Zsolnai, J. Organomet. Chem. 282 (1985) 331.

[10] G. Renner, P. Kircher, G. Huttner, P. Rutsch, K. Heinze, Eur. J. Inorg. Chem. (2000) 879.

[11] A.R. Rossi, R. Hoffmann, Inorg. Chem. 14 (1975) 365.

[12] (a) M. Veith, S. Becker, V. Huch, Angew. Chem. Int. Ed. Engl. 29 (1990) 216;

(b) M.F. Lappert, P.B. Hitchcock, S.A. Thomas, A.J. Thorne, A.J. Carty, N.T. Taylor, J. Organomet. Chem. 315 (1986) 27;

(c) A. Habbou, C. Lecomte, Acta Crystallogr. C48 (1992) 921;

(d) D. Lei, M.J. Hampden-Smith, E.N. Duesler, Polyhedron 9 (1990) 1127.

[13] (a) P.B. Hitchcock, M.F. Lappert, M.J. McGeary, Organometallics 9 (1990) 884;

(b) J.J. Schneider, N. Czap, D. Blaser, R. Boese, J. Am. Chem. Soc. 121 (1999) 1409;

(c) J.M Barbe, C. Guitard, C. Lecomte, R. Gerardin, Polyhedron 3 (1984) 889;

(d) J.J. Schneider, N. Czap, D. Blaser, R. Boese, J. Ensling, P. Outlich, C. Jariak, Chem. Eur. J. 6 (2000) 468.

[14] D.D. Perrin, W.L.F. Armarego, D.R. Perrin, Purification of Laboratory Chemicals, Pergamon Press, New York, 1985.

[15] G.M. Sheldrick, Acta Crystallogr. Sect. A 46 (1990) 467.

[16] G.M. Sheldrick, SHELXL-97, Program for Crystal Structure Refinement, University of Göttingen, Germany, 1997.

[17] GAUSSIAN-98, Revision A.7: M.J. Frisch, G.W. Trucks, H.B. Schlegel, G.E. Scuseria, M.A. Robb, J.R. Cheeseman, V.G. Zakrzewski, J.A. Montgomery, R.E. Stratman, J.C. Burant, S. Dapprich, J.M. Millam, A.D. Daniels, K.N. Kudin, M.C. Strain, O. Farkas, J. Tomasi, V. Barone, M. Cossi, R. Cammi, B. Mennucci, C. Pomelli, C. Adamo, S. Clifford, J. Ochterski, G.A. Petersson, P.Y. Ayala, Q. Cui, K. Morokuma, D.K. Malick, A.D. Rabuck, K. Raghavachari, J.B. Foresman, J. Cioslowswi, J.V. Ortiz, A.G. Baboul, B.B. Stefanov, G. Liu, A. Liashenko, P. Piskorz, I. Komaromi, R. Gomperts, R. Martin, D.J. Fox, T. Keith, M.A. Al-Laham, C.Y. Peng, A. Nanayakkara, C. Gonzalez, M. Challacombe, P.M.W. Gill, B. Jonhson, W. Chen, M.W. Wong, J.L. Andres, M. Head-Gordon, E.S. Replogle, J.A. Pople, Gaussian Inc., Pittsburgh PA, 1998.

[18] W.J. Hehre, L. Radom, P.V.R. Schleyer, J.A. Pople, Ab Initio Molecular Orbital Theory, Wiley, New York, 1986.

[19] R.G. Parr, W. Yang, in: R. Breslow, J.B. Goodenough (Eds.), Functional Theory of Atoms and Molecules, Oxford University Press, New York, 1989.

[20] (a) A.D. Becke, Phys. Rev. A38 (1988) 3098;

(b) A.D. Becke, J. Chem. Phys. 98 (1993) 5648;

(c) C. Lee, W. Yang, R.G. Parr, Phys. Rev. B37 (1988) 785.

[21] (a) W.J. Stevens, H. Basch, M. Krauss, J. Chem. Phys. 81 (1984) 6026;

(b) W.J. Stevens, H. Basch, M. Krauss, P. Jasien, Can. J. Chem. 79 (1992) 612;

(c) T.R. Cundari, W.J. Stevens, J. Chem. Phys. 98 (1993) 5555.

[22] (a) G.A. Petersson, M.A. Al-Laham, J. Chem. Phys. 94 (1991) 6081;

(b) G.A. Petersson, A. Bennett, T.G. Tensfeldt, M.A. Al-Laham, W.A. Shirley, J. Mantzaris, J. Chem. Phys. 89 (1988) 2193.

[23] (a) A.E. Reed, L.A. Curtiss, F.J. Weinhold, Chem. Rev. 88 (1988) 899;

(b) J.P. Foster, F. Weinhold, J. Am. Chem. Soc. 102 (1980) 7211.